Brightness enhancement of a multi-mode ribbon fiber using transmitting Bragg gratings

B. M. Anderson,[1,*] G. Venus,[1] D. Ott,[1] I. Divliansky,[1] J. W. Dawson,[2] D. R. Drachenberg,[2] M. J. Messerly,[2] P. H. Pax,[2] J. B. Tassano,[2] and L. B. Glebov[1]

[1]CREOL, The College of Optics and Photonics, University of Central Florida, P.O. Box 162700, Orlando, FL 32816, USA

[2] Lawrence Livermore National Lab, L-491, P.O. Box 808, Livermore, California 94551, USA

ABSTRACT

Increasing the dimensions of a waveguide provides the simplest means of reducing detrimental nonlinear effects, but such systems are inherently multi-mode, reducing the brightness of the system. Furthermore, using rectangular dimensions allows for improved heat extraction, as well as uniform temperature profile within the core. We propose a method of using the angular acceptance of a transmitting Bragg grating (TBG) to filter the fundamental mode of a fiber laser resonator, and as a means to increase the brightness of multi-mode fiber laser. Numerical modeling is used to calculate the diffraction losses needed to suppress the higher order modes in a laser system with saturable gain. The model is tested by constructing an external cavity resonator using an ytterbium doped ribbon fiber with core dimensions of 107.8μm by 8.3μm as the active medium. We show that the TBG increases the beam quality of the system from M^2 = 11.3 to M^2 = 1.45, while reducing the slope efficiency from 76% to 53%, overall increasing the brightness by 5.1 times.

Keywords: Volume Bragg grating, transverse mode, resonator, ribbon fiber, PTR glass

1. INTRODUCTION

Power scaling in narrow linewidth fiber lasers is frequently limited due to several detrimental nonlinear effects, such as stimulated Brillouin scattering (SBS), stimulated Raman scattering (SRS) and thermal lensing [1-3]. Increasing the mode area of a fiber allows for the intensity driven nonlinear effects to be minimized, allowing for increased output power. However, ultimately the fiber will be limited by thermal effects [2, 3]. To allow for improved heat extraction and uniform temperature profiles, 'ribbon' fibers with rectangular cores have been proposed [4]. The increased area of the core allows for decreased nonlinear effects, while the high aspect ratio of the fiber allows for a larger surface area to volume ratio for improved thermal performance. However, current designs of the fiber allow for multiple guided modes within the core, hurting the beam quality and brightness of the output. As a method of improving the brightness of multi-mode fibers lasers with high aspect ratios, we propose using the angular selectivity of transmitting Bragg grating to provide sufficient losses for the higher order modes to allow only the fundamental mode to be guided.

Many methods of filtering the fundamental mode in a fiber laser exist, but many of these have limited applicability to ribbon fibers or are ineffective in filtering the modes in short fiber resonators (high gain/length) due to their relatively small losses per length of fiber. Coiling the fiber has gain industry wide adoption, but has reduced effectiveness for core diameters beyond 40μm [5]. Coiling also can't be used for a ribbon fiber, where the intent is to coil the fiber along the single-mode axis for cooling purposes. Specialty fibers, such as leaky channel or other semi-guiding fibers can filter higher order modes in ribbon fibers, but depend on the higher order modes being filtered along the length of the fiber, and are less effective for very short fibers [6, 7]. Alternatively, excitation and amplification of a pure higher order mode has proven to be effective, and methods exist to convert this higher order mode into a Gaussian beam with high beam quality [4, 8].

We present a method of selecting the fundamental mode based on the angular selectivity of volume Bragg gratings (VBGs) recorded in photo-thermo-refractive (PTR) glass [9] which was successfully demonstrated in semiconductor, solid state lasers and fiber lasers [10-12]. Such a system can filter the higher order modes in the near field, allowing for high beam quality independent of cavity length. We present theoretical results modeling a ribbon fiber with saturable gain to estimate the angular selectivity needed for single-mode output, and the impact on

Fiber Lasers XII: Technology, Systems, and Applications, edited by L. Brandon Shaw, John Ballato,
Proc. of SPIE Vol. 9344, 93441W · © 2015 SPIE · CCC code: 0277-786X/15/$18 · doi: 10.1117/12.2079358

efficiency this will. We further present experimental results measuring the beam quality and efficiency as a function of angular selectivity in an external cavity resonator using an Yb-doped ribbon fiber as the gain medium.

2. THEORY

2.1 Volume Bragg gratings

Volume Bragg gratings are holographically recorded in a photosensitive glass known as photo-thermo-refractive glass (PTR) [9]. Exposure to near UV radiation followed by thermal development results in refractive index changes up to 1000 ppm (δn is about 10^{-3}). A two beam interference pattern is then used to create a sinusoidal modulation within the PTR glass to form the volume Bragg grating.

Theoretical modeling of volume Bragg gratings has been analytically described by Kogelnik by way of coupled-wave theory [13]. For a transmitting Bragg grating oriented 90° to the normal of the surface (symmetric TBG), the ratio of the scattered amplitude to the incident amplitude (S) is given as function of the dephasing (ξ) from the Bragg condition and the grating strength (ν) (Eq. 1). The diffraction efficiency for a plane wave is therefore the amplitude squared of S. The dephasing term (Eq. 2) shows the change in the diffraction efficiency as the incident plane wave makes small deviations from the Bragg condition, and is a function of the Bragg period (Λ_B), the angular deviation (δθ) from the Bragg angle (θB) in the medium, and the thickness of the grating (d). The grating strength (Eq. 3) controls the maximum diffraction efficiency, and is a function of the peak to peak refractive index modulation (δn), the grating thickness, the wavelength (λ) in the medium, and the Bragg angle in the medium. For a grating strength of ν = π/2, the diffraction efficiency is 100%. In general for a symmetric TBG, the angular acceptance is proportional to the ratio of the Bragg period to the grating thickness (Λ_B/d), while the peak diffraction efficiency is related to $\sin(\nu)^2$.

$$S = -ie^{-i\xi d}\left(\frac{\sin\left(\sqrt{\xi^2+\nu^2}\right)}{\sqrt{1+\frac{\xi^2}{\nu^2}}}\right) \tag{1}$$

$$\xi = \frac{2\pi}{\Lambda_B}\delta\theta d \tag{2}$$

$$\nu = \frac{\pi\delta n}{\lambda\cos(\theta_B)}d \tag{3}$$

For determining the interaction of a finite beam with a grating, plane wave decomposition is used [14, 15]. These theories allow for the description of the diffraction efficiency of a VBG interacting with the Hermite-Gaussian modes of a stable resonator, the LP modes of a circular core fiber, or any arbitrary wavefront. Formulation of this theory is shown in equations (4) – (7): (1) the Fourier transform is taken of the spatial distribution of the electric field to determine the far field angular distribution, (2) the angular distribution is multiplied with plane-wave response of the VBG, and (3) the inverse Fourier transform is taken to give the spatial distribution of the electric field after interaction with the grating.

$$E_{i,diff}(x,y,d) = \int_{-\infty}^{\infty}\int_{-\infty}^{\infty}\tilde{E}_i(k_x,k_y)S_{TBG}e^{-i\left(xk_x+yk_y+d\sqrt{1-k_x^2-k_y^2}\right)}dk_x\,dk_y \tag{4}$$

$$\tilde{E}_i(k_x,k_y) = \int_{-\infty}^{\infty}\int_{-\infty}^{\infty}E_i(x,y,0)e^{i(xk_x+yk_y)}dx\,dy \tag{5}$$

$$\eta_{eff,i} = \frac{\int_{-\infty}^{\infty}\int_{-\infty}^{\infty}\left|E_{i,diff}(x,y,d)\right|^2 dxdy}{\int_{-\infty}^{\infty}\int_{-\infty}^{\infty}|E_i(x,y,0)|^2 dxdy} \tag{6}$$

$$\eta_{i,j} = \frac{\left|\int_{-\infty}^{\infty}\int_{-\infty}^{\infty}E_{i,diff}^*(x,y)E_j(x,y)dxdy\right|^2}{\int_{-\infty}^{\infty}\int_{-\infty}^{\infty}\left|E_{i,diff}\right|^2 dxdy\int_{-\infty}^{\infty}\int_{-\infty}^{\infty}\left|E_j\right|^2 dxdy} \tag{7}$$

2.2 Laser gain and mode competition

Many models of mode competition and laser gain exist for fibers with circular symmetry. In particular, Gong, et al [16] have studied this process in multi-mode fibers while Huo and Cheo [17, 18] have studied multi-core fibers. These formulations have been adapted to the ribbon fiber which does not have circular symmetry, and are based on the steady state, space dependent rate equations formulated by Kelson and Hardy [18].

The three level rate steady state rate equations for the pump and signal are shown in equations (8) and (9). The forward (+) and backwards (-) traveling pump power (P_p) depends on the fill-factor (Γ_p) of the pump over the doped core, the emission (σ_{ep}) and the absorption (σ_{ap}) cross-sections in Yb^{3+} at the pump wavelength, the population inversion (N_{2j}, N_{1j}) in each core *j*, and the loss per unit length of the cladding guided pump (α_p). The signal power (P_{si}) of each mode *i*, depends on the fill-factor (Γ_{ij}) of mode *i* in core *j*, the emission (σ_{es}) and absorption (σ_{as}) cross-sections in Yb^{3+} at the signal wavelength, and the population inversion (N_{2j}, N_{1j}) in each core *j*, and the scattering losses (α_{si}) of each mode *i*.

The population inversions in each core must satisfy the steady state condition shown in equation (10), where A is the total area of the core, h is Plank's constant, and ν_p and ν_s are the pump and signal wavelengths respectively. Secondly, the doping population density in each core must be conserved, meaning $N_j = N_{1j} + N_{2j}$.

$$\pm\frac{dP_p^{\pm}}{dz} = \sum_j \Gamma_p\left(\sigma_{ep}N_{2j}(z) - \sigma_{ap}N_{1j}(z)\right)P_p^{\pm}(z) - \alpha_p P_p^{\pm}(z) \tag{8}$$

$$\pm\frac{dP_{si}^{\pm}(z)}{dz} = \sum_j \Gamma_{ij}\left(\sigma_{es}N_{2j}(z) - \sigma_{as}N_{1j}(z)\right)P_{si}^{\pm}(z) - \alpha_{si}P_{si}^{\pm}(z) \tag{9}$$

$$\left\{\frac{\Gamma_p\sigma_{ap}\left(P_p^p(z)+P_p^-(z)\right)}{A_k h\nu_p} + \sum_i \frac{\Gamma_{ij}\sigma_{as}\left(P_{si}^+(z)+P_{si}^-(z)\right)}{A_k h\nu_s}\right\}N_{1j}(z) \tag{10}$$

$$-\left\{\frac{\Gamma_p\sigma_{ep}\left(P_p^p(z)+P_p^-(z)\right)}{A_k h\nu_p} + \sum_i \frac{\Gamma_{ij}\sigma_{es}\left(P_{si}^+(z)+P_{si}^-(z)\right)}{A_k h\nu_s} + \frac{1}{\tau}\right\}N_{2j}(z) = 0$$

Given this setup, z = 0 is defined to be the location where the pump is coupled into the fiber, while z = L is the tip of the fiber where the output coupler resides. This means the initial pump in the fiber is equal to the pump coupled into the fiber ($P_p^+(0) = \eta_p P_{p,0}$ and $P_p^-(0) = 0$), while the signal is perfectly reflected and recoupled into the fiber minus Fresnel losses ($P_{si}^+(0) = 0.96^2 P_{si}^-(0)$). For the multi-mode resonator, no modal dependent losses exist, and the modes are equally recoupled into the fiber given the reflectivity of the output coupler ($P_{si}^-(L) = 0.04P_{si}^+(L)$). In the single mode case, the spatial filtering of the TBG causes modal dependent losses ($\eta_{eff,1,i}$) for the first pass, separate modal dependent losses for the second pass through the TBG ($\eta_{eff,2,i}$) as well as distortions which effects the recoupling of the modes ($\eta_{i,j}$) ($P_{si}^-(L) = 0.04\eta_{i,j}\eta_{eff,1,i}\eta_{eff,2,i}P_{si}^+(L)$). Output power of the system only has a single pass through the TBG, and is therefore given by the relation: $P_{out} = \sum_i 0.96\eta_{eff,1,i}P_{si}^+(L)$.

3. MODELING AND RESONATOR DESIGN

3.1 Guided modes and interaction with VBG

The quasi-TE guided modes of the ribbon fiber were calculated using a finite-difference solver of Maxwell's equations [19]. The refractive index was modeled after the ribbon fiber used in the experiments, 13 circular cores with diameter of 8.3 μm and a refractive index of $2.54*10^{-3}$ above the cladding index of 1.45 were sampled on the afore mentioned grid. The refractive index along the edge of the circular core was averaged to account for the gridding.

The near field and far field intensity distribution of several modes are shown in Figure 1.In the near field distributions, we see that small ripples are visible in the fundamental mode due to the shape of the core, although the electric field has flat phase fronts. Higher order modes follow the expected patterns, and have *i* π phase

discontinuities equal to the mode number *i*. The 13th mode has the largest overlap with the core, as each phase discontinuity matches the shape of the core, and is therefore expected to have the highest gain overlap.

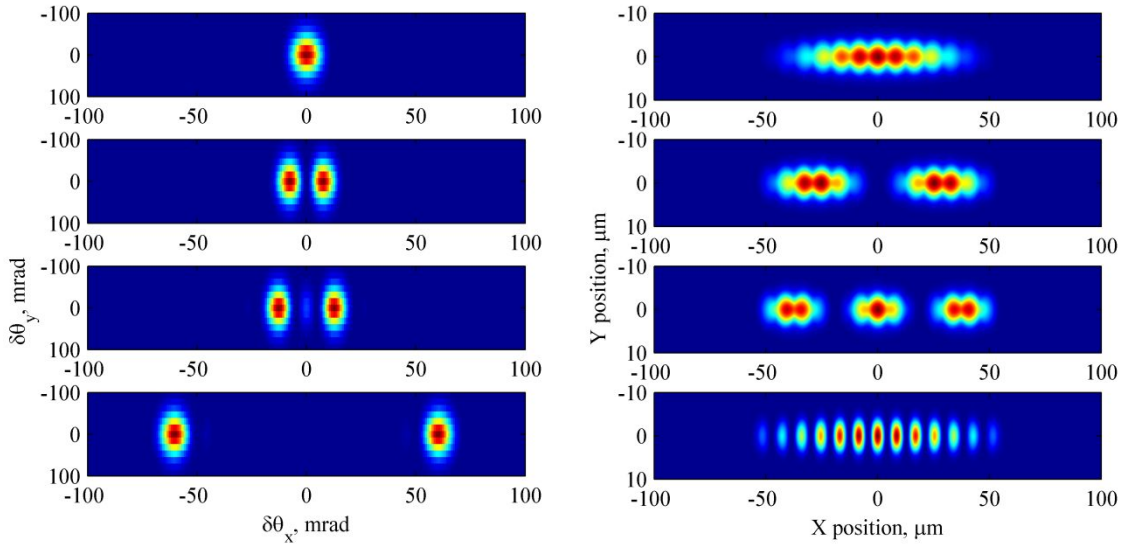

Figure 1: Calculated 2D intensity distributions for the 0th, 1st, 2nd and 12th modes shown in the near field (left) and far field (right).

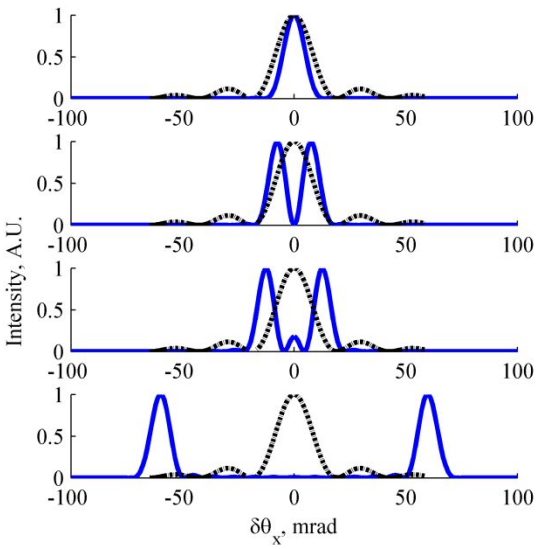

Figure 2: Calculated far field intensity distributions for the 0th, 1st, 2nd and 12th modes shown as 1-D cross sections (solid) overlayed with the angularly dependent diffraction efficiency of a TBG with FWHM of 17.4mrad (dashed). Due to the two lobes seen in the far field for higher order modes, only the fundamental mode has good overlap with the angular selectivity of the TBG.

The far field pattern of the fundamental mode shows that despite the ripples seen in the near field, the far field retains a nearly Gaussian appearance. The fundamental mode has a divergence of approximately 17.4 mrad, while the next highest order mode is approximately 2 times this. The nth higher order mode has a two lobed appearance in the far field, with the two lobes approximately spaced n times the fundamental mode divergence. This higher angular divergence allows them to be spatially filtered by the TBG.

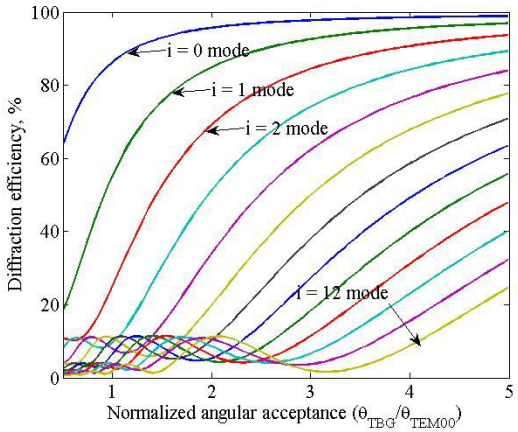

Figure 3: Single-pass diffraction efficiency of the guided ribbon-fiber modes as a function of angular selectivity for the TBG.

Calculations of the diffraction efficiency for a single pass through the TBG are found using equation 6, and are plotted in Figure 3. For a normalized angular acceptance of 5, the fundamental mode has low losses with ~99% diffraction efficiency, while significantly higher losses can be seen for all higher order modes. When the angular acceptance of the TBG is reduced to twice the divergence of the fundamental mode, diffraction efficiency remains >95%, while diffraction efficiency for the i=1 mode is reduced to <85%. In a resonator, this contrast in modal losses is expected to only allow the fundamental mode to oscillate within the system.

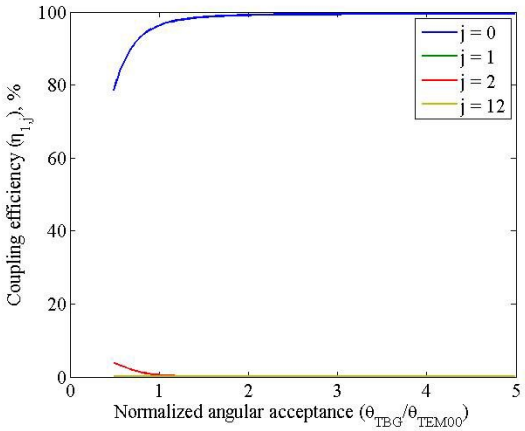

Figure 4: Coupling efficiency of the diffracted i = 0 mode into the j^{th} guided mode. High self-coupling and low cross-coupling is needed to retain high modal purity and beam quality.

The cross-coupling efficiency was calculated for each of the diffracted modes using equation (7). Plots of the coupling efficiency for the fundamental mode (i = 0) into each of the guided modes are shown in Figure 4. For very wide angular acceptance, the fundamental mode has very high coupling into the fundamental mode, indicating minimal distortions to the phase and intensity profile. As the angular acceptance is decreased, the coupling efficiency decreases. At the other extreme end, when the angular acceptance equals the divergence of the fundamental mode, the diffracted mode begins to couple into even numbered higher order modes.

From these calculations, it is therefore expected that there is both an upper-limit and lower limit where the TBG resonator is expected to be single-mode. For a TBG with too large an angular acceptance, losses are too low for the higher order modes, while for an angular acceptance which is too low, cross-coupling of the fundamental mode into the higher order modes is expected to reduce beam quality.

3.2 Cavity design

Using the framework shown, a linear oscillator using Yb-doped ribbon fiber was modeled, and the output power of each mode was measured. The parameters used are shown below in Table 1. For comparison, both the multi-mode oscillator and single-mode TBG resonator were modeled. The single-mode resonator was studied both with low power (8.4W absorbed pump and 1.0m of fiber) and high power (1000W of absorbed pump and 5.0m of fiber) to understand how gain saturation affects the modal content of the oscillator.

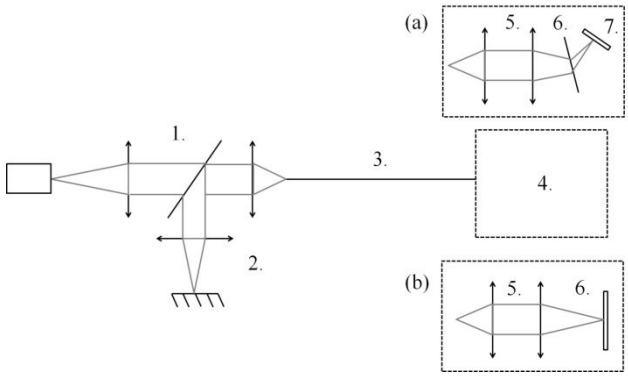

Figure 5: Block diagram of fiber laser with external resonator for two different configurations. Common components consist of: 1) pump combining optics, 2) reimaging of fiber onto high reflective mirror, 3) Gain medium, ytterbium doped fiber, 4) output coupling. A) Single-mode operation using 5) magnification optics, 6) TBG mode selector aligned to the fundamental mode, 7) Output coupler aligned to normal of diffracted beam. B) Multi-mode operation using 5) magnification optics, 6) output coupler aligned for maximum emission.

Table 1: Table of parameters used to model ribbon fiber oscillator.

Modeling parameters			
σ_{as}	$5.3\ 10^{-27}\ m^2$	σ_{ap}	$2630\ 10^{-27}\ m^2$
σ_{es}	$303\ 10^{-27}\ m^2$	σ_{ep}	$2630\ 10^{-27}\ m^2$
λ_s	1064 nm	λ_p	976 nm
α_{si}	0.02 dB/km	α_p	7 dB/km
A_k	$700\ \mu m^2$	A_{clad}	$22000\ \mu m^2$
τ	1.1 ms	N_j	$1.8*10^{25}\ m^{-3}$

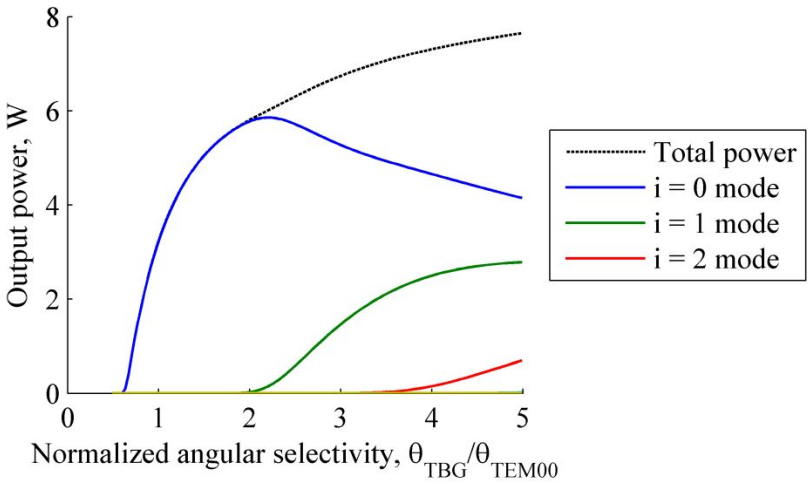

Figure 6: Modeling of the single mode resonator using 1.0m of fiber and 8.4W of absorbed pump power. The output powers for the first three modes are pictured as well as the total output power from the system. Single mode output can be obtained for a TBG angular selectivity 2 times larger than the divergence of the fundamental mode.

The ribbon fiber was first studied with low gain. A 1 m length of fiber was modeled with 8.4W of absorbed pump power. A TBG with angular acceptance ranging from 0.5 to 5.0 times the 17.4 mrad divergence of the fundamental mode was used as the mode selector. The modes and losses due to the TBG were previously calculated as shown in the previous section. The results of this modeling are plotted in Figure 7 showing the output power of each mode as well as the total output power from the system. The results of this modeling indicate the system will be effectively single mode for a normalized angular selectivity of between 0.5 and 2.0, while the fundamental mode will have a peak output for a normalized angular selectivity of 2.2. For large angular acceptance, fewer losses are seen for each mode, increasing the system efficiency but allowing higher order modes to oscillate in the system. For low angular acceptances, the TBG begins to cut into the fundamental mode, hurting efficiency but enhancing the brightness.

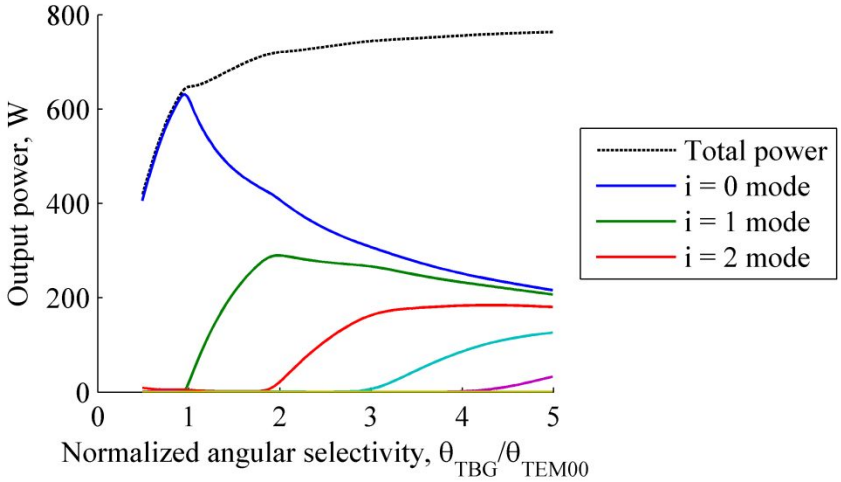

Figure 7 Output power of each mode using 1kW of pump power. Single mode output can be obtained when using a TBG with an angular acceptance equal to the divergence of the fundamental mode.

The single mode resonator was modeled for an optimal fiber length of 5.0m. A significantly larger incident pump of 1000W was modeled to show the effects of gain saturation. The results of this model are shown in Figure 7 detailing the output power of each mode as well at the total output power. With the increased pump power and higher gain saturation, higher modal losses are needed to suppress the high order modes, and the system will be single mode only for a normalized angular acceptance of between 0.5 and 0.95 times the divergence of the fundamental mode.

The fundamental mode has a peak output for an angular acceptance of approximately 0.95 (corresponding to 16.5 mrad), at which point 99% of the output power is in the fundamental mode and the total output power is 642 W. At this level of angular acceptance, a sharp increase in losses for the fundamental mode is seen, creating a narrow window at which the efficiency and brightness will be maximized (Figure 7).

4. EXPERIMENTAL RESULTS

A linear oscillator was constructed using a 1.0m section of an active ribbon fiber as the gain medium. A cross section of the fiber is shown in Figure 8. The core consists of 13 Yb^{3+} doped silica rods with dimensions of approximately 8.3 μm in diameter, and each have a refractive index of 2.54*10-3 above the silica cladding. The core dimensions are approximately 8.3 μm by 107.8 μm, while the inner diameter of the cladding is 167μm. The cladding absorption is approximately 2.2 dB/m at 915.

To study transverse mode selection in a ribbon fiber laser, the external resonator shown in Figure 5a was constructed and compared to the output from the multi-mode resonator shown in Figure 5b. The resonator is a linear cavity, with two sets of magnification optics to reimage the fiber facets onto the feedback mirrors. At the back end of the fiber, a high reflecting mirror is used for feedback and combined with the pump to be coupled into the fiber. At the front end of the fiber, the fiber modes are magnified by a factor of 6.7 and, for the single mode configuration, diffracted by a TBG. According to modeling, the fundamental mode is expected to have a divergence of approximately 2.6 mrad. The TBG is aligned to provide maximum diffraction efficiency for the fundamental mode. After diffraction, the Fresnel reflection from a wedge is used as an output coupler and aligned to provide maximum feedback for the fundamental mode. In this system, the magnification optics are only necessary to match the angular content of the fundamental mode with the angular selectivity of the TBG. Practical iterations of this system could implement an optimized TBG, and allow for many of the free space components to be removed.

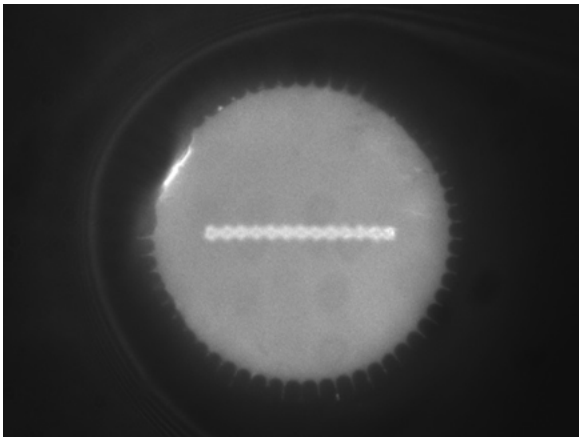

Figure 8: Microscopic image of an air clad, 13 core Yb-doped ribbon fiber. The core is approximately 107.8 μm along the slow axis and 8.3 μm in the fast axis.

The TBG used in the experiment had an angular selectivity varying from 1.8 mrad, 2.4 mrad, 4.7 mrad, and 7.1 mrad, and the diffraction efficiency of each was above 98% adding low losses to the system. The beam quality and slope efficiency was measured as a function of the angular selectivity in order to maximize the brightness of the system. With the wide angular selectivity, the beam quality was quite poor with an M^2 of 1.7, while the slope efficiency was quite high at 62%. Reducing the angular selectivity produced notable improvements in the beam quality as the side lobes disappear and the shape becomes more Gaussian. At 1.8mrad the beam is nearly diffraction limited with an M^2 of 1.1, although slope efficiency is nearly reduced to 20%, hurting the brightness of the system. Brightness is maximized between an angular selectivity of 2.4 mrad and 4.7 mrad, with 4.7 mrad producing slightly better output power with not much worse beam quality.

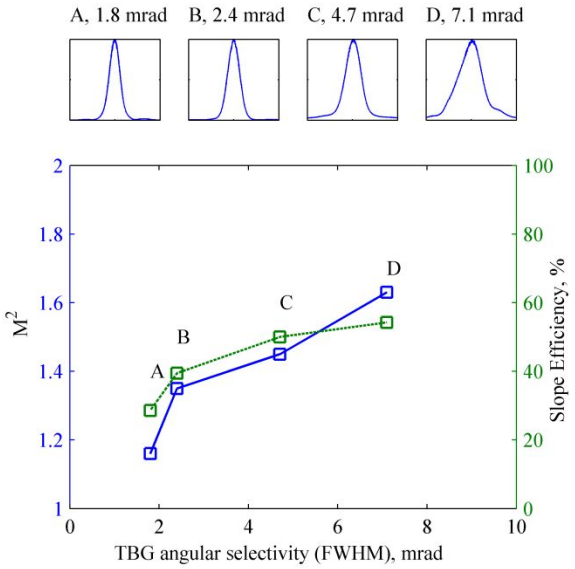

Figure 9: Slope efficiency and beam quality measurements made as a function of TBG angular selectivity. Brightness is maximized for the 4.7 mrad TBG.

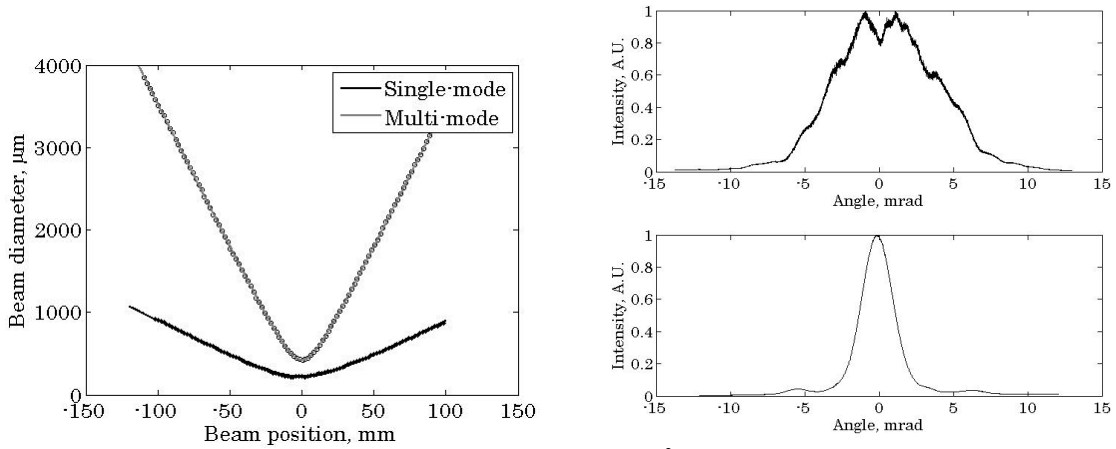

Figure 10: (Left) Comparison of beam quality for the multi-mode (M^2 = 11.3) and single mode using a TBG with 4.7 mrad angular selectivity (M^2 = 1.45) case (Right) comparison of the far field intensity showing the multi-mode and single-mode case.

Slope efficiency was measured and compared for the multi-mode and single-mode resonators, and is shown in Fig. 13. In the multi-mode system, the absorber power slope efficiency was of 76% with a threshold of 1.5 W, producing a maximum output power of 17.3 W for an absorbed power of 23.9 W and a brightness of 0.878 W/(mm^{2}mrad^2). In the single mode system, slope efficiency is reduced to 53% and threshold is increased to 1.9 W, giving a maximum output power of 11.3 W for an absorbed pump power of 23.7 W and a brightness of 4.45 W/(mm^{2}mrad^2). The single-mode beam was observed to be stable through the tested range. Some reduction in slope efficiency can be attributed to the features of the TBG used in the experiments. The TBG has a maximum diffraction efficiency of 98%, while the overlap with the fundamental is predicted to reduce the effective diffraction efficiency to 95%. Additional losses are being investigated. However, despite the additional losses, brightness was improved by a factor of 5.1 due to the dramatic improvement of beam quality. Notable in the measurement in the slope efficiency is that beam quality had no variations throughout the power range despite reaching more than 10x threshold.

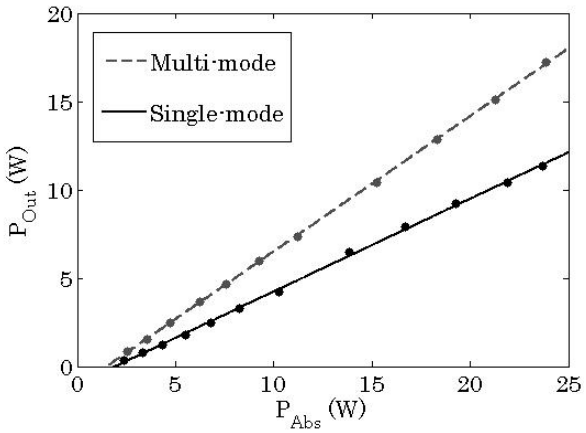

Figure 11: Comparison of absorbed power slope efficiencies for the multi-mode and single-mode systems. The dashed line represents the multimode cavity with a slope efficiency of 76%. The solid line represents the single-mode cavity with a slope efficiency of 53%.

5. CONCLUSION

In conclusion, we have proposed the use of a TBG has a near field spatial filter for use in a ribbon fiber laser with a high aspect ratio. We have built a theoretical laser model with saturable gain which allows us to understand the angular losses needed for single-mode operation and could allow us to optimize the system in the future. We have experimental verified this model, and found the TBG improved the beam quality by 7.8x and enhanced the brightness by 5.1x. Our model indicates the system should scale to higher pump powers of more than 1 kW without gain saturation or mode competition hurting the beam quality, although further models are needed to understand the nonlinear effects of the system. Ultimately, we believe this system will be important for the power scaling fiber oscillators, allowing for increased core sizes while maintaining high beam quality, with important implications for the design of resonators where the cavity length is important, such as single-frequency resonators or short pulse q-switched lasers.

REFERENCES

[1] Richardson, D. J., Nilsson, J., Clarkson, W. a., "High power fiber lasers: current status and future perspectives [Invited]," J. Opt. Soc. Am. B **27**(11), B63 (2010).

[2] Zhu, J., Zhou, P., Wang, X., Xu, X.., Liu, Z., "Analysis of Maximum Extractable Power of Fiber Sources," IEEE J. Quantum Electron. **48**(4), 480–484 (2012).

[3] Dawson, J. W., Messerly, M. J., Beach, R. J., Shverdin, M. Y., Stappaerts, E. a., Sridharan, A. K., Pax, P. H., Heebner, J. E., Siders, C. W., et al., "Analysis of the scalability of diffraction-limited fiber lasers and amplifiers to high average power.," Opt. Express **16**(17), 13240–13266 (2008).

[4] Drachenberg, D. R., Messerly, M. J., Pax, P. H., Sridharan, A., Tassano, J., Dawson, J., "First selective mode excitation and amplification in a ribbon core optical fiber," Opt. Express **21**(9), 11257–11269 (2013).

[5] Koplow, J. P., Kliner, D. A., Goldberg, L., "Single-mode operation of a coiled multimode fiber amplifier.," Opt. Lett. **25**(7), 442–444 (2000).

[6] Khitrov, V., Shkunov, V. V., Rockwell, D. A., Zakharenkov, Y. A.., Strohkendl, F., "Er- doped high aspect ratio core (HARC) rectangular fiber producing 5 -mJ , 13-nsec pulses at 1572 nm," Adv. Solid-State Photonics, 1–3 (2012).

[7] Russell, P. S. J., "Photonic-Crystal Fibers," J. Light. Technol. **24**(12), 4729–4749 (2006).

[8] Ishaaya, A. A., Machavariani, G., Davidson, N., Friesem, A. A., Hasman, E., "Conversion of a high-order mode beam into a nearly Gaussian beam by use of a single interferometric element.," Opt. Lett. **28**(7), 504–506 (2003).

[9] Glebov, L. "Photosensitive glass for phase hologram recording," Glass Sci. Technol. **71**, 85-90 (1998).

[10] Venus, G. B., Sevian, A., Smirnov, V. I.., Glebov, L. B., "High-brightness narrow-line laser diode source with volume Bragg-grating feedback," Proc. SPIE **5711**, 166–176 (2005).
[11] Glebov, L. "High-performance solid-state and fiber lasers controlled by volume Bragg gratings," Rev. of Laser Eng. **41**, 684-690 (2013).
[12] Anderson, B., Venus, G., Ott, D., Divliansky, I., Dawson, J. W., Drachenberg, D. R., Messerly, M. J., Pax, P. H., Tassano, J. B., et al., "Fundamental mode operation of a ribbon fiber laser by way of volume Bragg gratings," Opt. Lett. **39**(22), 6498–6500 (2014).
[13] Kogelnik, H., "Coupled Wave Theory for Thick Hologram Gratings," Bell Syst. Tech. J **48**(9), 2909–2947 (1969).
[14] Hsieh, H., Liu, W., Havermeyer, F., Moser, C., Psaltis, D., "Beam-width-dependent filtering properties of strong holographic gratings," Appl. Opt. **45**(16), 3774–3780 (2006).
[15] Hellström, J. E., Jacobsson, B., Pasiskevicius, V., Laurell, F., "Finite Beams in Reflective Volume Bragg Gratings : Theory and Experiments," IEEE J. Quantum Electron. **44**(1), 81–89 (2008).
[16] Gong, M., Yuan, Y., Li, C., Yan, P., Zhang, H., Liao, S., "Numerical modeling of transverse mode competition in strongly pumped multimode fiber lasers and amplifiers," Opt. Express **15**(6), 3236–3246 (2007).
[17] Huo, Y., Cheo, P. K., "Analysis of transverse mode competition and selection in multicore fiber lasers," J. Opt. Soc. Am. B **22**(11), 2345 (2005).
[18] Kelson, I., Hardy, A. A., "Strongly Pumped Fiber Lasers," J. Quantum Electron. **34**(9), 1570–1577 (1998).
[19] Kawano, K., [Introduction to optical waveguide analysis], John Wiley & Sons, Inc, New York, 117-164, (2001).